The Astrophysical Journal, 796:57 (5pp), 2014 November 20 doi:10.1088/0004-637X/796/1/57

ISOTOPOLOGUES OF DENSE GAS TRACERS IN NGC 1068

Junzhi Wang[1,2], Zhi-Yu Zhang[3,4], Jianjie Qiu[1], Yong Shi[5], Jiangshui Zhang[6], and Min Fang[4,7]
[1] Shanghai Astronomical Observatory, Chinese Academy of Sciences, 80 Nandan Road, 200030, Shanghai, People's Republic of China; jzwang@shao.ac.cn
[2] Key Laboratory of Radio Astronomy, Chinese Academy of Sciences, 210008, Nanjing, People's Republic of China
[3] Institute for Astronomy, University of Edinburgh, Royal Observatory, Blackford Hill, Edinburgh EH9 3HJ, UK
[4] ESO, Karl Schwarzschild Strasse 2, D-85748 Garching bei Munich, Germany
[5] School of Astronomy and Space Science, Nanjing University, Nanjing, 210093, People's Republic of China
[6] Center For Astrophysics, GuangZhou University, 510006, GuangZhou, People's Republic of China
[7] Departamento de Física Teórica, Universidad Autónoma de Madrid, Cantoblanco 28049, Madrid, Spain
Received 2014 March 6; accepted 2014 September 18; published 2014 November 5

ABSTRACT

We present observations of isotopic lines of dense gas tracers toward the nuclear region of nearby Seyfert 2 galaxy NGC 1068 with the IRAM 30 m telescope and the Atacama Pathfinder Experiment (APEX) 12 m telescope. We detected four isotopic lines ($H^{13}CN$ 1–0, $H^{13}CO^+$ 1–0, $HN^{13}C$ 1–0, and $HC^{18}O^+$ 1–0) at the 3 mm band with the IRAM 30 m telescope and obtained upper limits of other lines. We calculated optical depths of dense gas tracers with the detected isotopic lines of HCN 1–0, HCO^+ 1–0, and HNC 1–0. We find that the $^{14}N/^{15}N$ abundance ratio is greater than 420 if we adopt the upper limit of $HC^{15}N$(1–0) emission. Combining this with fluxes of 1–0 lines from IRAM 30 m observations and the upper limit of 3–2 lines from APEX 12 m observations, we also estimated the excitation condition of molecular gas in the nuclear region of NGC 1068, which is less dense than that in the extreme starburst regions of galaxies.

Key words: galaxies: active – galaxies: individual (NGC 1068) – galaxies: ISM

Online-only material: color figures

1. INTRODUCTION

Molecular gas in galaxies is an important material reservoir not only for forming stars but also for fueling the central supermassive black holes of active galactic nuclei (AGNs). The total molecular gas in galaxies is normally traced by low-J transition CO lines (Young & Scoville 1991). In active star-forming regions and circumnuclear disks (CNDs) near AGNs, molecular gas with a density higher than 10^4 cm^{-3} is the key for understanding the star formation process and physical properties in the CNDs. The dense molecular gas is traced by transitions of molecules with high dipole moments such as HCN (1–0) (Gao & Solomon 2004). However, CO lines and the dense gas tracers (HCN, CS, HCO^+, and HNC, etc.) are normally optically thick, which causes large uncertainty in estimating the mass of the molecular gas, even with observations of multiple transitions (Papadopoulos et al. 2012). Multiple transitions of isotopic lines of CO, e.g., ^{13}CO and $C^{18}O$, which are often optically thin, can be used to better estimate molecular gas mass and excitation conditions in galaxies. ^{13}CO lines have been observed in several samples of local galaxies (Aalto et al. 1991; Casoli et al. 1992; Garay et al. 1993; Glenn & Hunter 2001; Tan et al. 2011) and even in strongly lensed high-z galaxies (Danielson et al. 2013). Due to their weakness, isotopic lines of dense gas tracers have been detected in only a few very nearby galaxies (Henkel et al. 1998; Chin et al. 1999; Wang et al. 2004; Aladro et al. 2013). With new measurements of dense gas tracers and their isotopologues, it is possible to obtain their optical depths under the reasonable assumptions of isotopic abundance ratios. This can better estimate dense gas mass in galaxies than only estimate it with the total flux of optically thick dense gas tracers.

As a Seyfert 2 galaxy at a distance of 14.4 Mpc ($1'' = 72$ pc; Bland-Hawthorn et al. 1997), NGC 1068 has a circumnuclear molecular ring with two bright knots and two spiral arms with a diameter of $\sim 40''$ (Schinnerer et al. 2000). Most of star formation activities take place in the two spiral arms, while the circumnuclear ring is mainly affected by the central AGN (Usero et al. 2004; Tsai et al. 2012). The high ratio of the brightness–temperature of CO(3–2)/(1–0) (3.12 ± 0.03) was found in the nuclear region with observations of the Submillimeter Array and OVRO (Tsai et al. 2012). This means that the physical conditions in the CND of NGC 1068 are different from those in the star-forming regions, where the CO(3–2)/(1–0) ratio is normally less than unity (Yao et al. 2003). Such a high ratio can be explained by a gas component of low opacity and high density, which is higher than the critical density of CO(3–2) (Tsai et al. 2012). With multiple transitions of the dense gas tracers (HCN, HNC, and HCO^+) and their isotopic lines, it is possible to determine the physical properties (density, temperature, mass, etc.) of most important parts of the molecular gas near the central AGN and better understand the effect of nuclear activity on the ISM.

In this paper, we describe observations made with the IRAM 30 m and Atacama Pathfinder Experiment (APEX) 12 m telescopes and data reduction in Section 2. We present the main results in Section 3, discussion in Section 4, and a brief summary in Section 5.

2. OBSERVATIONS AND DATA REDUCTION

2.1. IRAM 30 m Observations

We observed NGC 1068 with the IRAM 30 m telescope at Pico Veleta, Spain,[8] in 2011 December. We adopt a standard wobbler switching mode with a $\pm 120''$ offset at a 0.5 Hz beam throwing. The Eight Mixer Receiver with dual polarization and the Fast Fourier Transform Spectrometer (FTS) backend with $\sim$8 GHz frequency coverage and 195 kHz frequency spacing, which corresponds to about

[8] Based on observations carried out with the IRAM 30 m telescope. IRAM is supported by INSU/CNRS (France), MPG (Germany), and IGN (Spain).

0.67 km s^{-1} at 87 GHz, were used for these observations. The observed frequency ranges from ~84.2 GHz to ~92.2 GHz, which covers three dense gas tracers and their isotopic lines: HCN(1–0), HCO$^+$(1–0), HNC(1–0), H^{13}CN(1–0), HC^{15}N(1–0), H^{13}CO$^+$(1–0), HC^{18}O$^+$(1–0), HC^{17}O$^+$(1–0), H^{15}NC(1–0), and HN^{13}C(1–0). The typical system temperature is about 120 K. Pointing and focusing were checked about every 2 hr with nearby strong millimeter-emitting quasi-stellar objects. The total ON+OFF source time was about 15 hr. As we pointed the telescope to the center of this galaxy and the beam size of IRAM 30 m telescope is about 29″ at 90 GHz, most of the detected emission is from the circumnuclear region instead of the two spiral arms of NGC 1068.

2.2. APEX Observations

Our 1 mm observations were performed in 2012 September with the APEX on the Chajnantor Plateau in Chile in good (pwv ~ 1.8–2.3 mm) weather conditions. The Swedish Heterodyne Facility Instrument (SHeFI) was employed to observe H^{13}CN(3–2), H^{13}CO$^+$(3–2), HN^{13}C(3–2), and HC^{15}N(3–2) simultaneously. The typical system temperature was about 250 K. The FTS backends led to a bandwidth of 4 GHz with a channel spacing of 0.076 mHz. The beam size was ~23.″5 at 260 GHz.

All observations were performed in wobbler switching mode with a beam-throwing distance of 4′. Every 10 minutes, we made a chopper wheel calibration. The focus was determined on Saturn. Pointing was checked and calibrated on O-Ceti once per hour, resulting in a typical uncertainty of 2″–3″ (rms). Including overhead, we spent ~4 hr of telescope time.

2.3. Data Reduction

All the data were reduced with the CLASS package of GILDAS.[9] We inspected each spectrum visually and qualified spectra by comparing the measured noise and the theoretical noise before and after a few applications of boxcar smoothing. None of the IRAM 30 m spectra and about 5% of the APEX spectra were discarded during the qualification. We subtracted linear baselines for all spectra and averaged them with time weighting.

3. RESULTS

With the IRAM 30 m telescope, we detected H^{13}CN(1–0), H^{13}CO$^+$(1–0), HC^{18}O$^+$(1–0), and HN^{13}C(1–0) lines in NGC 1068, which are listed in Table 1 and presented in Figure 1. The rms level in $T_{\rm mb}$ is about 0.25 mK after being smoothed to a velocity resolution of ~28 km s^{-1} (see Figure 1). Other isotopic lines, i.e., HC^{15}N(1–0), HC^{17}O$^+$(1–0), and H^{15}NC(1–0), are not detected with the IRAM 30 m telescope. We only obtained upper limits of H^{13}CN(3–2), H^{13}CO$^+$(3–2), HN^{13}C(3–2), and HC^{15}N(3–2) with APEX 12 m telescope. The rms level is about 1 mK in $T_{\rm mb}$ after being smoothed to a velocity resolution of ~57 km s^{-1} (see Figure 2). For lines with non-detection, we estimate upper limits of the velocity-integrated fluxes using the line widths of related isotopic lines and their noises, which are also listed in Table 1.

Among our detected lines, the HC^{18}O$^+$(1–0) line is detected for the first time in NGC 1068, while detections of other lines have been reported in Aladro et al. (2013). With four times better sensitivity, our data can not only better derive the velocity-integrated fluxes of the isotopic lines, but they can also be useful for comparing line profiles with their major isotopologues obtained simultaneously. Among the isotopic lines of dense gas tracers, H^{13}CN(1–0) is the strongest one. However, the line flux, line center, and line width of our ^{13}C isotopologues have significant differences from those in Costagliola et al. (2010), but are consistent with the line flux results from Costagliola et al. (2010).

The H^{13}CO$^+$(1–0) line is blended with SiO J = 2–1 (v = 0) and HCO (1–0). With three Gaussian components fitting, we obtain a more accurate flux of H^{13}CO$^+$(1–0) than that from Aladro et al. (2013). For the H^{13}CO$^+$(1–0) spectrum presented in Figure 1, emission of SiO J = 2–1 (v = 0) and HCO(1–0) have been removed with fitting results using the "residual" command in CLASS. Compared with the HCO$^+$(1–0) line, H^{13}CO$^+$(1–0) was found to be broader and blueshifted, which is due to the contamination from the non-Gaussian emission components of SiO J = 2–1 (v = 0) at the blue part of H^{13}CO$^+$(1–0) emission (see Figure 1), which may cause overestimation of line flux. The ratios of the velocity-integrated fluxes of HCN(1–0)/H^{13}CN(1–0), HCO$^+$(1–0)/H^{13}CO$^+$(1–0), and HNC(1–0)/HN^{13}C(1–0) are 16.1, 19.7, and 38.1, respectively, while they were 16.1, 17.1, and 23.3, respectively, in Aladro et al. (2013). The large difference in the HNC(1–0) to HN^{13}C(1–0) ratio is likely due to low signal-to-noise ratio (S/N) data (~1σ) in Aladro et al. (2013).

Table 1
Observed Isotopic Lines of Dense Gas Tracers in NGC 1068

Transition	Frequency (GHz)	Flux (mK km s^{-1})	Velocity (km s^{-1})	Line Width (km s^{-1})
HCN(1–0)	88.632	20578.6 ± 44.9	1150.8 ± 0.2	249.3 ± 0.5
H^{13}CN(1–0)	86.340	1282.3 ± 33.5	1109.3 ± 2.7	215.6 ± 6.5
HC^{15}N(1–0)	86.055	<115(2σ)		
HCO$^+$(1–0)	89.189	14430.9 ± 66.5	1167.7 ± 0.6	244.1 ± 1.2
H^{13}CO$^+$(1–0)	86.754	734.4 ± 38.2	1124.9 ± 6.9	270.5 ± 15.8
HC^{18}O$^+$(1–0)	85.162	133.1 ± 36.8	1124.5 ± 49.5	300.8 ± 83.3
HC^{17}O$^+$(1–0)	87.057	<144(2σ)		
HNC(1–0)	90.664	7781.6 ± 35.5	1186.0 ± 0.6	243.5 ± 30.0
HN^{13}C(1–0)	87.091	204.2 ± 28.5	1117.5 ± 16.2	216.3 ± 30.8
H^{15}NC(1–0)	88.866	<112(2σ)		
HC^{15}N(3–2)	258.157	<460(2σ)		
H^{13}CN(3–2)	259.012	<460(2σ)		
HN^{13}C(3–2)	261.263	<450(2σ)		
H^{13}CO$^+$(3–2)	260.255	<570(2σ)		

Note. The fluxes are from the Gaussian fitting.

4. DISCUSSION

4.1. Comparison of Dense Gas Tracers with Their Isotopologues

In Table 1, we list the properties of three molecules (HCN, HNC, and HCO$^+$) and their isotopologues. All detected isotopic lines are at the 3 mm band. We overlay the spectra of HCN(1–0), HNC(1–0), and HCO$^+$(1–0) on the detected isotopic lines: H^{13}CN(1–0), HN^{13}C(1–0), H^{13}CO$^+$(1–0), and HC^{18}O$^+$(1–0) in Figure 1, and find different line profiles between dense gas tracers and their isotopologues. The lines with good S/N can be used to determine line profiles for such a comparison. At the rms noise level of ~0.25 mK, line profiles of dense gas tracers and the two strong isotopic lines (H^{13}CO$^+$(1–0) and H^{13}CN(1–0)) can be well defined, while it is difficult to constrain the line profile of the marginal detected line HC^{18}O$^+$(1–0). The

[9] http://www.iram.fr/IRAMFR/GILDAS

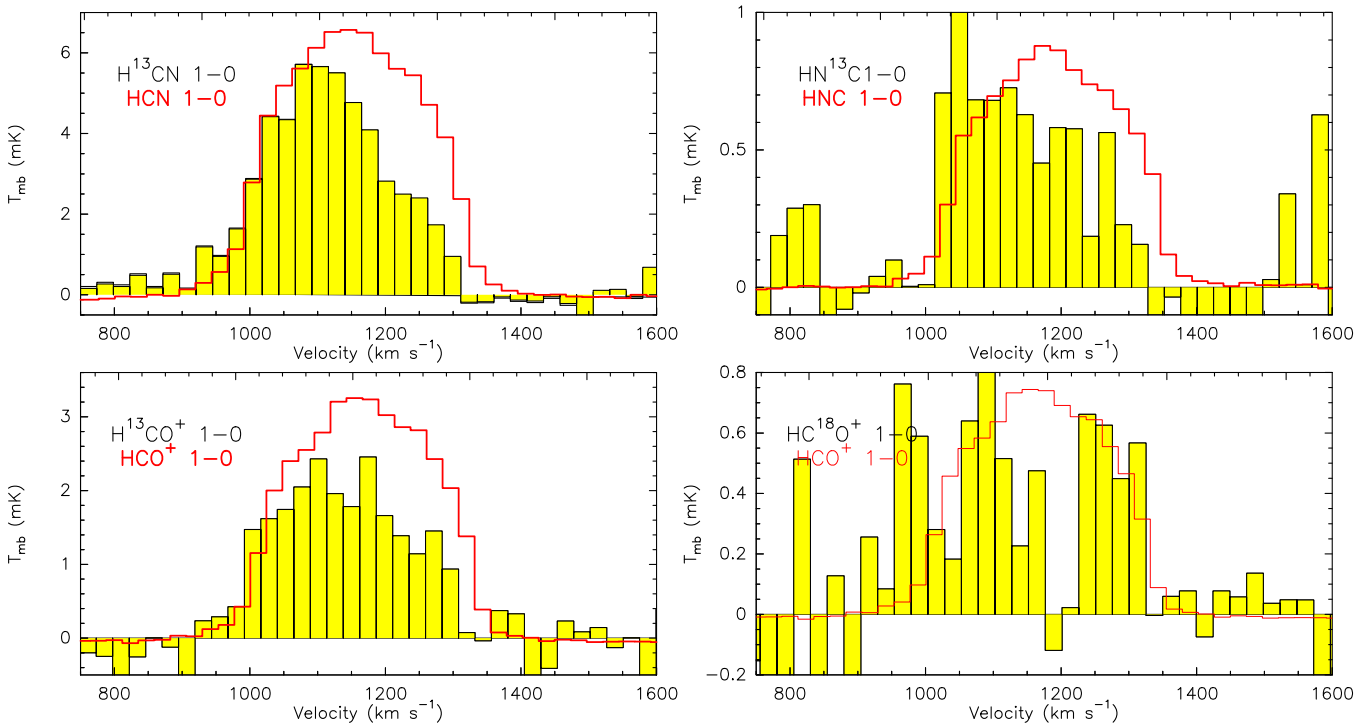

Figure 1. Top left: $H^{13}CN(1–0)$ overlaid with HCN(1–0) (divided by 11); top right: $HN^{13}C(1–0)$ overlaid with HNC(1–0) (divided by 35); bottom left: $H^{13}CO^{+}(1–0)$ overlaid with $HCO^{+}(1–0)$ (divided by 16); and bottom right: $HC^{18}O^{+}(1–0)$ overlaid with $HCO^{+}(1–0)$ (divided by 70).
(A color version of this figure is available in the online journal.)

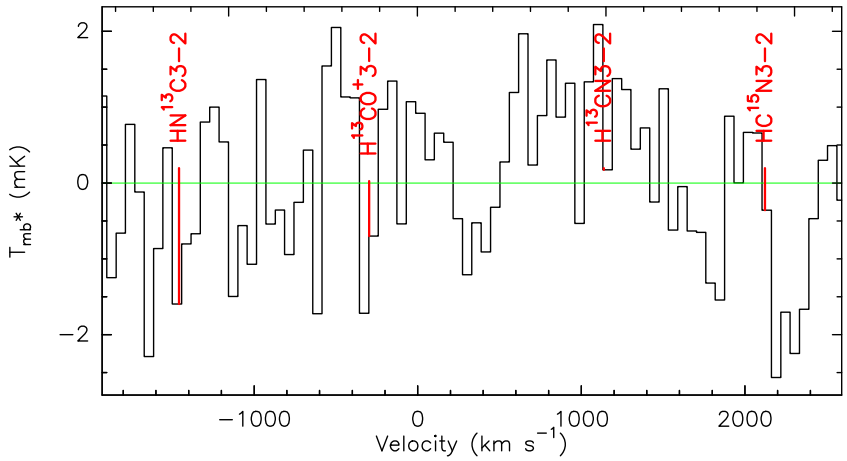

Figure 2. Observed spectrum around 260 GHz, which covers $H^{13}CN(3–2)$, $H^{13}CO^{+}(3–2)$, $HN^{13}C(3–2)$, and $HC^{15}N(3–2)$ with non-detection.
(A color version of this figure is available in the online journal.)

dense gas tracers show non-Gaussian but similar line profiles (see Figure 3). The profile of our high quality HNC(1–0) line is not consistent with that in Pérez-Beaupuits et al. (2007), which was obtained with SEST. However, our HNC detection is consistent with the general results of Huettemeister et al. (1995), observed with IRAM 30 m telescope. When the S/N is low, it is hard to see the deviation from a Gaussian profile like what had been shown for HNC(1–0) in Huettemeister et al. (1995), and also $H^{13}CO^{+}(1–0)$ and $H^{13}CN(1–0)$ in Figure 1. To check such a trait, we select a subset of our HCN (1–0) data using, which is about 5 minutes of on-source time, to do simple component Gaussian fitting. The fitted result does not show obvious deviation from a Gaussian profile. Therefore, even though the differences between $H^{13}CO^{+}(1–0)$ and $HCO^{+}(1–0)$ and between $H^{13}CN(1–0)$ and HCN(1–0) are obvious, it is hard to say that the isotopic lines have well-defined single Gaussian profiles.

Comparing the line profiles of dense gas tracers with their isotopic lines (see Figure 1), we find that the blueshifted parts have smaller ratios of dense gas tracers to their ^{13}C isotopic lines than the redshifted parts. Assuming a homogeneously $^{12}C/^{13}C$ abundance in different parts of NGC 1068, the different line ratios are due to optical depth effect: the redshifted parts have lower optical depths. We can tell from high-resolution observations with BIMA, most of the HCN(1–0) emission is from the nuclear regions instead of the two arms, where there exists a large amount of molecular gas with strong CO(1–0) emission (Helfer & Blitz 1995). From spatially resolved data, the HCN(1–0) spectrum at the nuclear region peaks at the velocity of ∼1100 km s^{-1} (Helfer & Blitz 1995), which is similar to

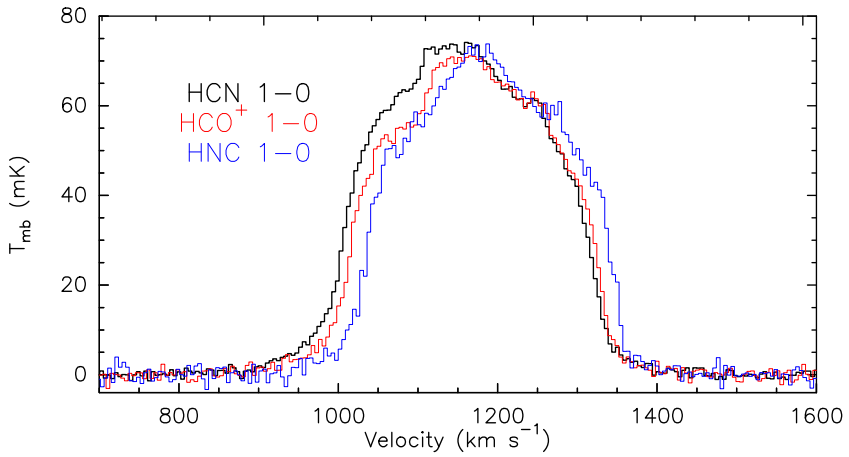

Figure 3. HCN(1–0) (black), HCO^+(1–0) (red, ×(4/3)), and HNC(1–0) (blue, ×2.5) spectra of NGC 1068 observed by the IRAM 30 m telescope.
(A color version of this figure is available in the online journal.)

the peak of our $H^{13}CN$(1–0) spectrum, but not consistent with our HCN(1–0) spectrum obtained with large beam size (see Figure 1 and Table 1). Therefore, the optically thin HCN(1–0) and HCO^+(1–0) emissions are more likely from the spiral arms instead of the nuclear region. Based on this, we use the ratios of dense gas tracers and their isotopes (11 for HCN, 16 for HCO^+, and 35 for HNC) to match the profiles at the blueshifted side instead of velocity-integrated flux to calculate the optical depths of dense gas tracers in the nuclear region.

Assuming the $^{12}C/^{13}C$ abundance ratios are the same for all the dense gas tracers in NGC 1068, we can obtain a lower limit of this ratio. Such an abundance ratio should be higher than the line ratios, which are 16 for HCN(1–0)/$H^{13}CN$(1–0), 20 for HCO^+(1–0)/$H^{13}CO^+$(1–0), 38 for HNC(1–0)/$HN^{13}C$(1–0), and the $^{12}C/^{13}C$ abundance ratio was suggested to be ∼40 for nearby starburst galaxies (Henkel et al. 1995). We adopted a number of 49, which was obtained with the line ratio of CN(1–0)/^{13}CN(1–0) in Aladro et al. (2013) as the $^{12}C/^{13}C$ abundance ratio in the nuclear region of NGC 1068. Otherwise, if we use 40 as the abundance ratio, the HNC(1–0) will be almost optically thin, which is not likely to be true. Using the relation of $R = (1 - e^{-\tau_{12}})/(1 - e^{-\tau_{13}})$, where R is the line ratio and τ is the optical depth, we obtained the optical depths of HCN(1–0), HCO^+(1–0), and HNC(1–0) to be 4.6, 3.0, and 0.73, respectively.

4.2. Isotopic Abundance Ratios and Excitation Conditions of Dense Gas in the Nuclear Region of NGC 1068

With upper limits of the ^{15}N species, the line ratio of $H^{13}CN$(1–0)/$HC^{15}N$(1–0) should be higher than 11 using 2σ as upper limit of $HC^{15}N$(1–0). Since both lines are optically thin and have similar critical densities, the line ratio is directly linked to the abundance ratio of $H^{13}CN/HC^{15}N$. Since the lower limit of the $^{12}C/^{13}C$ abundance ratio obtained with the flux ratio of HNC(1–0)/$HN^{13}C$(1–0) is 38.1, the $^{14}N/^{15}N$ abundance ratio is greater than $38.1 \times 11 = 419$. With the $^{12}C/^{13}C$ ratio of 49, we find that the $^{14}N/^{15}N$ abundance ratio is greater than 539, which is much higher than that in the local interstellar medium value of 290 ± 30 (Adande & Ziurys 2012), but similar to that in the center of our Galaxy (Wilson & Rood 1994). On the other hand, based on the $H^{13}CO^+$(1–0)/$HC^{18}O^+$(1–0) ratio and the assumed $^{12}C/^{13}C$ ratio of 49, we obtained the $^{16}O/^{18}O$ ratio to be 270, similar to that in the Galactic center (Henkel & Mauersberger 1993).

With the non-detections of $J = 3$–2 transition isotopic lines at 1 mm, we obtain the upper limits of 3–2/1–0 line ratios for $H^{13}CN$, $H^{13}CO^+$, and $HN^{13}C$, which indicates that the $J = 3$ levels of these molecules do not reach thermal equilibrium (TE). Under the TE condition for lines from the same molecule at different transitions, the optical depth and the brightness temperature are larger at higher transitions than lower transitions. The optical depth τ is $\propto n_u A_{ul}(e^{(h\nu/kT_{ex})} - 1)$, where n_u is the number of molecules at the upper level, A_{ul} is the Einstein A coefficient of the transition, h is the Planck constant, ν is the line frequency, k is the Boltzmann constant, and T_{ex} is the excitation temperature. The ratio of number density at the upper level to that at the ground state is $n_u/n_0 = (g_u/g_0)e^{-(E_u/kT_{ex})}$, where g is the statistical weight and E_u is the energy from the upper level to the ground state. For $T_{ex} = 20$ K, n_3/n_1 is about 0.8, while A_{3-2}/A_{1-0} is about 35 from CDMS (http://www.astro.uni-koeln.de/cgi-bin/cdmssearch) for the $H^{13}CN$ molecule. With $T_{ex} = 20K$, $(e^{(h\nu/kT_{ex})} - 1)$ is 0.87 and 0.23 for $H^{13}CN$ 3–2 and 1–0, respectively. If $H^{13}CN$ is thermalized, the ratio of optical depths between $H^{13}CN$ 3–2 and 1–0 is about 100. When the volume density of molecular gas is less than the critical density of specified transition, such a ratio will be lower than that under the TE condition. If lines at both transitions are optically thin, the line ratio in brightness–temperature should be the same as the optical depth ratio. Based on our observations with the IRAM 30 m and APEX 12 m telescopes (see Table 1), the line ratio of $H^{13}CN$ 3–2/1–0 in NGC 1068 is less than 0.25 after being converted to the same beam size in brightness–temperature. For comparison, the line ratio of $H^{13}CN$ 3–2/1–0 is about 15 for Orion in the unit of brightness–temperature (Turner 1989; Blake et al. 1986). Thus most of the molecular gas in the nuclear region of NGC 1068 is below the critical density of high transition dense gas tracers, which means that the molecular gas is less dense than that in the extreme nuclear starbursts, such as Arp 220, which shows the $H^{13}CN$ (3–2)/(1–0) ratio near unity in brightness–temperature (J. Wang et al., in preparation).

5. SUMMARY

With observations of isotopic lines of dense gas tracers toward the nuclear region of nearby gas-rich Seyfert 2 galaxy NGC 1068 with the IRAM 30 m and APEX 12 m telescopes, we detected four isotopic lines of dense gas tracers: $H^{13}CN$(1–0),

$HN^{13}C$(1–0), $H^{13}CO^+$(1–0), and $HC^{18}O^+$(1–0). $HC^{18}O^+$(1–0) was detected for the first time in this source as a marginal detection, while our $HN^{13}C$ 1–0 shows different flux and line center to those reported in Aladro et al. (2013). We calculated the optical depth of the dense gas tracers with the detected isotopic lines, which are 4.6 for HCN(1–0), 3.0 for HCO^+(1–0), and 0.73 for HNC(1–0) with the assumption of $^{12}C/^{13}C = 49$. $^{14}N/^{15}N$ abundance ratio was estimated to be greater than 420, with an upper limit of the $HC^{15}N$(1–0) line, while the derived $^{16}O/^{18}O$ ratio is about 270. The non-detection of 1 mm isotopic lines indicated that the molecular gas in the nuclear region of NGC 1068 is less dense than that in extreme starburst regions of galaxies.

This work is partly supported by the China Ministry of Science and Technology under the State Key Development Program for Basic Research (2012CB821800) and partly supported by the Natural Science Foundation of China under grants 11173013 and 11178009. We thank the staff at the IRAM 30 m and APEX telescopes for their kind help and support during our observations. Z.Y.Z. acknowledges support from the European Research Council (ERC) in the form of Advanced Grant COSMICISM.

REFERENCES

Aalto, S., Johansson, L. E. B., Booth, R. S., & Black, J. H. 1991, A&A, 249, 323
Adande, G. R., & Ziurys, L. M. 2012, ApJ, 744, 194
Aladro, R., Viti, S., Bayet, E., et al. 2013, A&A, 549, A39
Blake, G. A., Masson, C. R., Phillips, T. G., & Sutton, E. C. 1986, ApJS, 60, 357
Bland-Hawthorn, J., Gallimore, J. F., Tacconi, L. J., et al. 1997, Ap&SS, 248, 9
Casoli, F., Dupraz, C., & Combes, F. 1992, A&A, 264, 55
Chin, Y.-N., Henkel, C., Langer, N., & Mauersberger, R. 1999, ApJL, 512, L143
Costagliola, F., Aalto, S., Rodriguez, M. I., et al. 2011, A&A, 528, 30
Danielson, A. L. R., Swinbank, A. M., Smail, Ian, Bayet, E., et al. 2013, MNRAS, 436, 2793
Gao, Y., & Solomon, P. M. 2004, ApJ, 606, 271
Garay, G., Mardones, D., & Mirabel, I. F. 1993, A&A, 277, 405
Glenn, J., & Hunter, T. R. 2001, ApJS, 135, 177
Helfer, T. T., & Blitz, L. 1995, ApJ, 450, 90
Henkel, C., Chin, Y.-N., Mauersberger, R., & Whiteoak, J. B. 1998, A&A, 329, 443
Henkel, C., & Mauersberger, R. 1993, A&A, 274, 730
Henkel, C., Mauersberger, R., Wiklind, T., et al. 1993, A&A, 268, L17
Huettemeister, S., Henkel, C., Mauersberger, R., et al. 1995, A&A, 295, 571
Papadopoulos, P. P., van der Werf, P., Xilouris, E., Isaak, K. G., & Gao, Y. 2012, ApJ, 751, 10
Pérez-Beaupuits, J. P., Aalto, S., & Gerebro, H. 2007, A&A, 476, 177
Schinnerer, E., Eckart, A., Tacconi, L. J., Genzel, R., & Downes, D. 2000, ApJ, 533, 850
Tan, Q., Gao, Y., Zhang, Z., & Xia, X. 2011, RAA, 11, 787
Tsai, M., Hwang, C.-Y., Matsushita, S., Baker, A. J., & Espada, D. 2012, ApJ, 749, 129
Turner, B. E. 1989, ApJS, 70, 539
Usero, A., García-Burillo, S., Fuente, A., Martín-Pintado, J., & Rodríguez-Fernández, N. J. 2004, A&A, 419, 897
Wang, M., Henkel, C., Chin, Y.-N., et al. 2004, A&A, 422, 883
Wilson, T. L., & Rood, R. 1994, ARA&A, 32, 191
Yao, L., Seaquist, E. R., Kuno, N., & Dunne, L. 2003, ApJ, 588, 771
Young, J. S., & Scoville, N. Z. 1991, ARA&A, 29, 581